Interleukin-6 is an activator of pituitary stem cells upon local damage, a competence quenched in the aging gland

Peer-reviewed author version

Vennekens, A; Laporte , E; HERMANS, Florian; Cox , B; Modave, E; Janiszewski, A; Nys, C; Kobayashi, H; Malengier-Devlies, B; Chappell, J; Matthys , P; Garcia, MI; Pasque, V; Lambrechts, D & Vankelecom, H (2021) Interleukin-6 is an activator of pituitary stem cells upon local damage, a competence quenched in the aging gland. In: Proceedings of the National Academy of Sciences of the United States of America, 118 (25) (Art N° e2100052118).

DOI: 10.1073/pnas.2100052118
Handle: http://hdl.handle.net/1942/35883

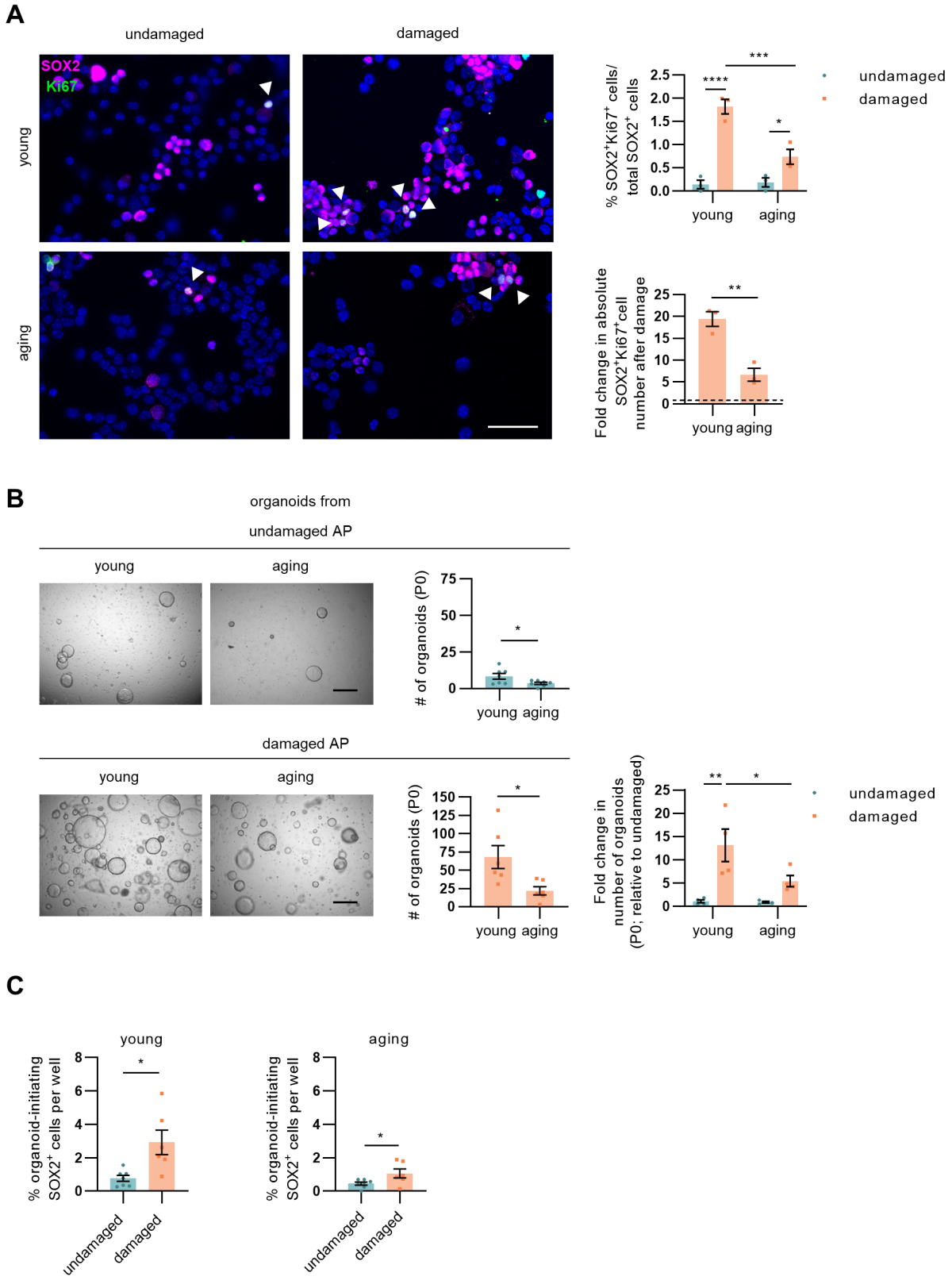
A
undamaged
damaged
SOX2
Ki67
young
aging
% SOX2+Ki67+ cells/ total SOX2+ cells
2.5
2.0
1.5
1.0
0.5
0.0
****
***
*
young
aging
undamaged
damaged
Fold change in absolute SOX2+Ki67+cell number after damage
25
20
15
10
5
0
**
young aging
B
organoids from
undamaged AP
young
aging
# of organoids (P0)
75
50
25
0
*
young aging
damaged AP
young
aging
# of organoids (P0)
150
125
100
75
50
25
0
*
young aging
Fold change in number of organoids (P0; relative to undamaged)
25
20
15
10
5
0
**
*
young
aging
undamaged
damaged
C
young
% organoid-initiating SOX2+ cells per well
8
6
4
2
0
*
undamaged
damaged
aging
% organoid-initiating SOX2+ cells per well
8
6
4
2
0
*
undamaged
damaged

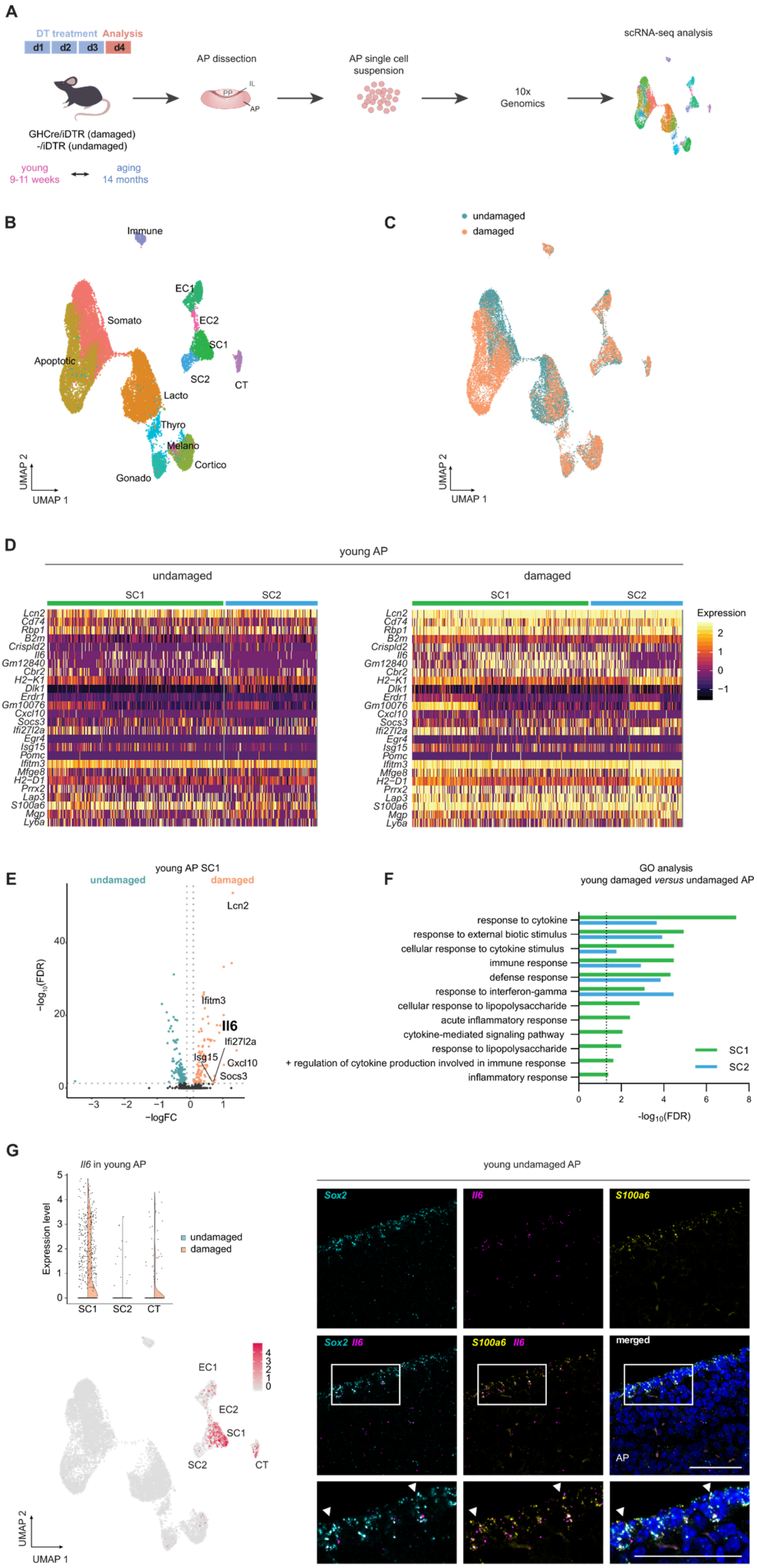
A
DT treatment
Analysis
d1
d2
d3
d4
GHCre/iDTR (damaged)
-/iDTR (undamaged)
young
9-11 weeks
aging
14 months
AP dissection
PP
IL
AP
AP single cell suspension
10x Genomics
scRNA-seq analysis
B
Immune
EC1
EC2
SC1
SC2
CT
Somato
Apoptotic
Lacto
Thyro
Melano
Cortico
Gonado
UMAP 2
UMAP 1
C
undamaged
damaged
UMAP 2
UMAP 1
D
young AP
undamaged
damaged
SC1
SC2
Lcn2
Cd74
Rbp1
B2m
Crispld2
Il6
Gm12840
Cbr2
H2-K1
Dlk1
Erdr1
Gm10076
Cxcl10
Socs3
Ifi27l2a
Egr4
Isg15
Pomc
Ifitm3
Mfge8
H2-D1
Prrx2
Lap3
S100a6
Mgp
Ly6a
Expression
2
1
0
−1
E
young AP SC1
undamaged
damaged
Lcn2
Ifitm3
Il6
Ifi27l2a
Isg15
Cxcl10
Socs3
−log10(FDR)
−logFC
F
GO analysis
young damaged versus undamaged AP
response to cytokine
response to external biotic stimulus
cellular response to cytokine stimulus
immune response
defense response
response to interferon-gamma
cellular response to lipopolysaccharide
acute inflammatory response
cytokine-mediated signaling pathway
response to lipopolysaccharide
+ regulation of cytokine production involved in immune response
inflammatory response
SC1
SC2
-log10(FDR)
G
Il6 in young AP
Expression level
undamaged
damaged
SC1
SC2
CT
EC1
EC2
SC1
SC2
CT
UMAP 2
UMAP 1
young undamaged AP
Sox2
Il6
S100a6
Sox2 Il6
S100a6 Il6
merged
AP

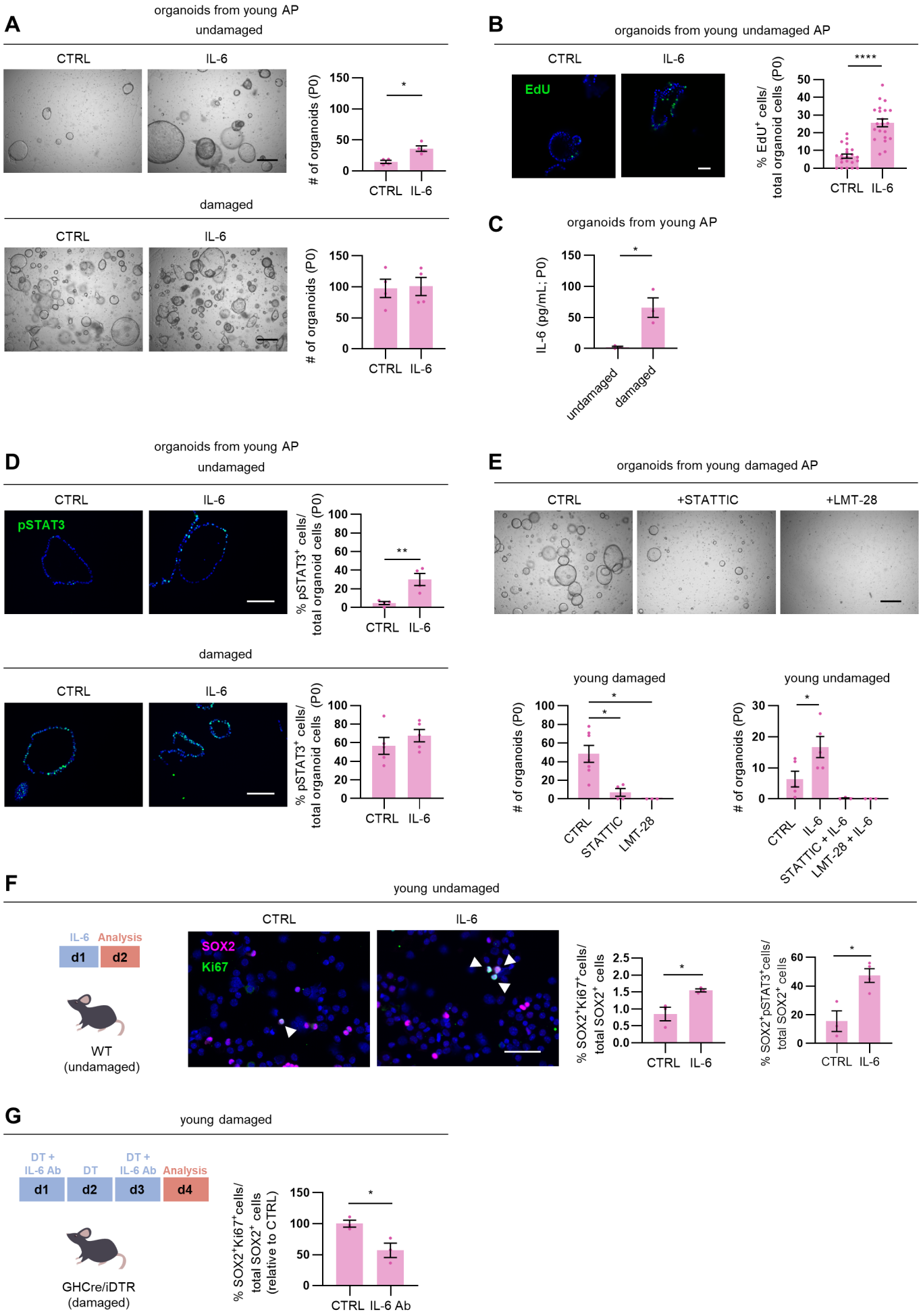
A
organoids from young AP
undamaged
CTRL
IL-6
# of organoids (P0)
150
100
50
0
*
CTRL IL-6
damaged
CTRL
IL-6
# of organoids (P0)
150
100
50
0
CTRL IL-6
B
organoids from young undamaged AP
CTRL
IL-6
EdU
% EdU+ cells/ total organoid cells (P0)
50
40
30
20
10
0
****
CTRL IL-6
C
organoids from young AP
IL-6 (pg/mL; P0)
150
100
50
0
*
undamaged
damaged
D
organoids from young AP
undamaged
CTRL
IL-6
pSTAT3
% pSTAT3+ cells/ total organoid cells (P0)
100
80
60
40
20
0
**
CTRL IL-6
damaged
CTRL
IL-6
% pSTAT3+ cells/ total organoid cells (P0)
100
80
60
40
20
0
CTRL IL-6
E
organoids from young damaged AP
CTRL
+STATTIC
+LMT-28
young damaged
# of organoids (P0)
100
80
60
40
20
0
*
*
CTRL
STATTIC
LMT-28
young undamaged
# of organoids (P0)
30
20
10
0
*
CTRL
IL-6
STATTIC + IL-6
LMT-28 + IL-6
F
young undamaged
IL-6
Analysis
d1
d2
WT
(undamaged)
CTRL
IL-6
SOX2
Ki67
% SOX2+Ki67+cells/ total SOX2+ cells
2.5
2.0
1.5
1.0
0.5
0.0
*
CTRL IL-6
% SOX2+pSTAT3+cells/ total SOX2+ cells
60
40
20
0
*
CTRL IL-6
G
young damaged
DT + IL-6 Ab
DT
DT + IL-6 Ab
Analysis
d1
d2
d3
d4
GHCre/iDTR
(damaged)
% SOX2+Ki67+cells/ total SOX2+ cells (relative to CTRL)
150
100
50
0
*
CTRL IL-6 Ab

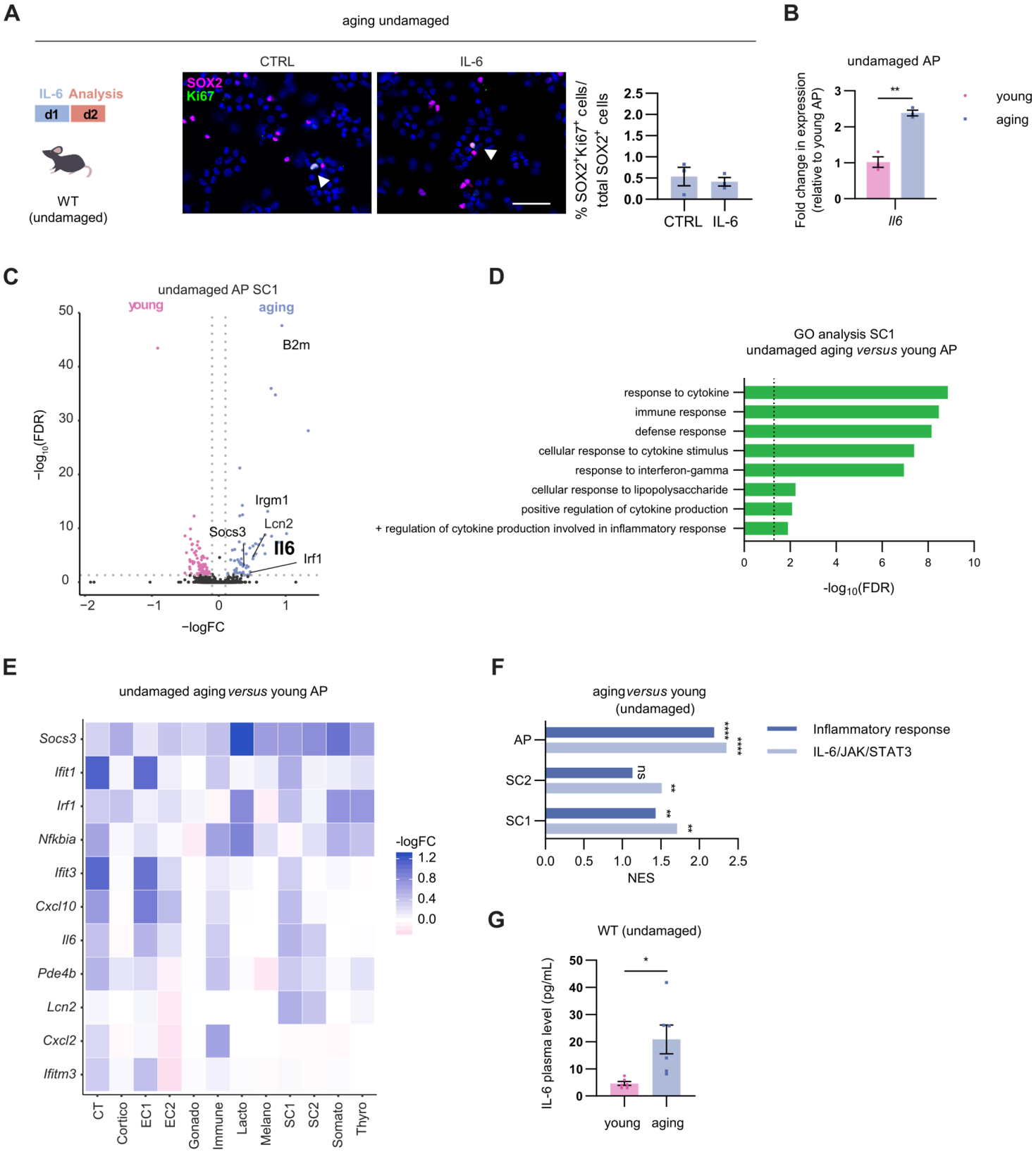
A
aging undamaged
IL-6 Analysis
d1
d2
WT
(undamaged)
CTRL
IL-6
SOX2
Ki67
% SOX2+Ki67+ cells/
total SOX2+ cells
2.5
2.0
1.5
1.0
0.5
0.0
CTRL
IL-6
B
undamaged AP
Fold change in expression
(relative to young AP)
3
2
1
0
**
Il6
young
aging
C
undamaged AP SC1
young
aging
B2m
Irgm1
Lcn2
Socs3
Il6
Irf1
−log10(FDR)
50
40
30
20
10
0
−2
−1
0
1
−logFC
D
GO analysis SC1
undamaged aging versus young AP
response to cytokine
immune response
defense response
cellular response to cytokine stimulus
response to interferon-gamma
cellular response to lipopolysaccharide
positive regulation of cytokine production
+ regulation of cytokine production involved in inflammatory response
0
2
4
6
8
10
-log10(FDR)
E
undamaged aging versus young AP
Socs3
Ifit1
Irf1
Nfkbia
Ifit3
Cxcl10
Il6
Pde4b
Lcn2
Cxcl2
Ifitm3
CT
Cortico
EC1
EC2
Gonado
Immune
Lacto
Melano
SC1
SC2
Somato
Thyro
-logFC
1.2
0.8
0.4
0.0
F
aging versus young
(undamaged)
AP
SC2
SC1
****
****
ns
**
**
**
0.0
0.5
1.0
1.5
2.0
2.5
NES
Inflammatory response
IL-6/JAK/STAT3
G
WT (undamaged)
IL-6 plasma level (pg/mL)
50
40
30
20
10
0
*
young
aging

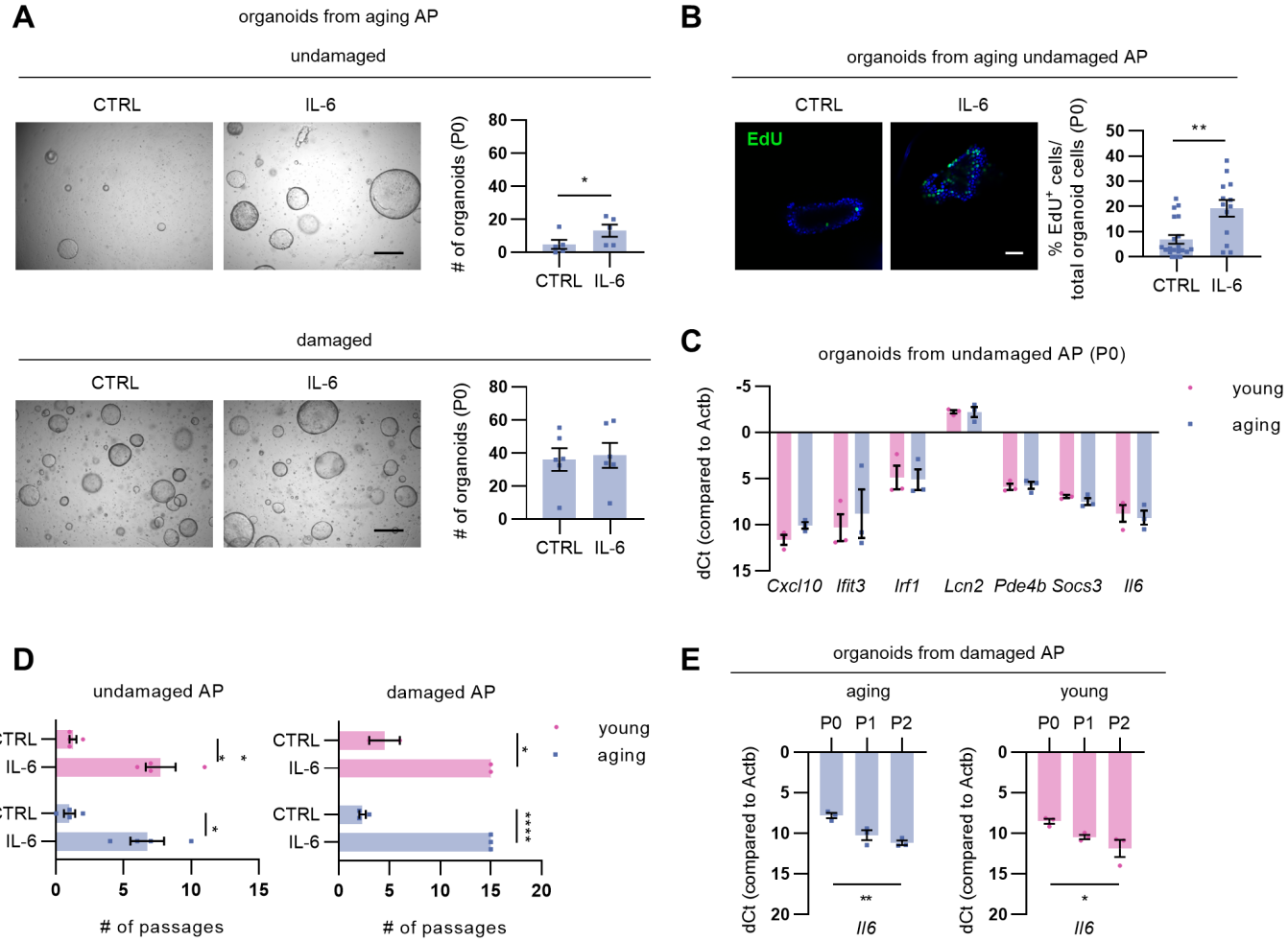
A
organoids from aging AP
undamaged
CTRL
IL-6
# of organoids (P0)
80
60
40
20
0
*
CTRL
IL-6
damaged
CTRL
IL-6
# of organoids (P0)
80
60
40
20
0
CTRL
IL-6
B
organoids from aging undamaged AP
CTRL
IL-6
EdU
% EdU+ cells/ total organoid cells (P0)
50
40
30
20
10
0
**
CTRL
IL-6
C
organoids from undamaged AP (P0)
young
aging
dCt (compared to Actb)
-5
0
5
10
15
Cxcl10
Ifit3
Irf1
Lcn2
Pde4b
Socs3
Il6
D
undamaged AP
damaged AP
young
aging
CTRL
IL-6
CTRL
IL-6
*
*
*
*
****
0
5
10
15
0
5
10
15
20
# of passages
# of passages
E
organoids from damaged AP
aging
young
P0
P1
P2
P0
P1
P2
dCt (compared to Actb)
0
5
10
15
20
**
*
Il6
Il6

PNAS
www.pnas.org

Main Manuscript for

Interleukin-6 is an activator of pituitary stem cells upon local damage, a competence quenched in the aging gland

Annelies Vennekens[1]*, Emma Laporte[1]*, Florian Hermans[1,2], Benoit Cox[1], Elodie Modave[3,4], Adrian Janiszewski[5], Charlotte Nys[1], Hiroto Kobayashi[1,6], Bert Malengier-Devlies[7], Joel Chappell[5], Patrick Matthys[7], Marie-Isabelle Garcia[8], Vincent Pasque[5], Diether Lambrechts[3,9], Hugo Vankelecom[1,#]

[1]Laboratory of Tissue Plasticity in Health and Disease, Cluster of Stem Cell and Developmental Biology, Department of Development and Regeneration, Leuven Stem Cell Institute, KU Leuven (University of Leuven), Leuven, Belgium
[2]Laboratory of Morphology, Biomedical Research Institute, Hasselt University, Diepenbeek, Belgium
[3]Center for Cancer Biology, VIB, Leuven, Belgium
[4]Laboratory for Intestinal Neuroimmune Interactions, Translational Research Center for Gastrointestinal Disorders, Department of Chronic Diseases, Metabolism and Ageing, KU Leuven, Leuven, Belgium
[5]Laboratory for Cellular Reprogramming and Epigenetic Regulation, Cluster of Stem Cell and Developmental Biology, Department of Development and Regeneration, Leuven Stem Cell Institute, KU Leuven, Leuven, Belgium
[6]Department of Anatomy and Structural Science, Yamagata University Faculty of Medicine, Yamagata, Japan
[7]Immunity and Inflammation Research Group, Department of Microbiology, Immunology and Transplantation, KU Leuven, Leuven, Belgium
[8]Institut de Recherche Interdisciplinaire en Biologie Humaine et Moléculaire (IRIBHM), Faculty of Medicine, Université Libre de Bruxelles (ULB), Brussels, Belgium
[9]Laboratory for Translational Genetics, Department of Human Genetics, KU Leuven, Leuven, Belgium

*Both authors contributed equally

[#]Corresponding author: Hugo Vankelecom

Email: hugo.vankelecom@kuleuven.be

Hugo Vankelecom: 0000-0002-2251-7284
Annelies Vennekens: 0000-0001-6278-251X
Emma Laporte: 0000-0003-0799-3116
Florian Hermans: 0000-0002-2321-3995
Benoit Cox: 0000-0002-3139-268X

Elodie Modave: 0000-0002-5775-3332
Adrian Janiszewski: 0000-0002-4156-5791
Charlotte Nys: 0000-0001-8917-7934
Bert Malengier-Devlies: 0000-0003-3527-1145
Joel Chappell: 0000-0002-5834-4100
Patrick Matthys: 0000-0002-9685-6836
Marie-Isabelle Garcia: 0000-0003-2147-7003
Vincent Pasque: 0000-0002-5129-0146
Diether Lambrechts: 0000-0002-3429-302X

Classification

Major category: Biological Sciences
Minor category: Cell Biology

Keywords

pituitary; stem cells; interleukin-6; aging; organoids

Author Contributions

A.V. and E.L. designed the concepts and experiments, performed the experiments, analyzed the data, interpreted the results and co-wrote the manuscript; F.H. processed scRNA-seq data and regulon analysis, and assisted in confocal imaging of organoids; B.C. provided pituitary organoid expertise and data, and assisted in experimental set-up; E.M. performed initial scRNA-seq bioinformatic processing; A.J. assisted in scRNA-seq analysis and co-performed regulon analysis; C.N. helped with specific organoid experiments; H.K. performed and co-interpreted transmission electron microscopy; B.M-D. assisted in immune cell- and cytokine-related analyses; J.C. assisted in scRNA-seq analysis; P.M. supervised immune cell- and cytokine-related analyses; M-I.G. contributed to specific immunostaining experiments; V.P. co-supervised scRNA-seq and regulon analysis; D.L. co-supervised scRNA-seq experiments and analysis; H.V. supervised the entire project, co-developed the concepts and ideas, co-designed the experiments, co-interpreted the data and wrote the manuscript. All authors critically reviewed and approved the manuscript.

This PDF file includes:

Main Text
Legends to Figures

Abstract

Stem cells in the adult pituitary are quiescent, yet show acute activation upon tissue injury. Molecular mechanisms underlying this reaction are completely unknown. We applied single-cell transcriptomics to start unraveling the acute pituitary stem cell activation process as occurring upon targeted endocrine cell-ablation damage. This stem cell reaction was contrasted to aging (middle-aged) pituitary, known to have lost damage-repair capacity.

Stem cells in aging pituitary show regressed proliferative activation upon injury and diminished *in vitro* organoid formation. Single-cell RNA sequencing (scRNA-seq) uncovered interleukin-6 (IL-6) as being upregulated upon damage, however only in young but not aging pituitary. Administering IL-6 to young mice promptly triggered pituitary stem cell proliferation, while blocking IL-6 or associated signaling pathways inhibited such reaction to damage. By contrast, IL-6 did not generate a pituitary stem cell activation response in aging mice, coinciding with elevated basal IL-6 levels and raised inflammatory nature in the aging gland (inflammaging). Intriguingly, *in vitro* stem cell activation by IL-6 was not only discerned in organoid culture from young but also aging pituitary, indicating that the aging gland's stem cells retain intrinsic activatability, *in vivo* likely impeded by the prevailing inflammatory tissue milieu. Importantly, IL-6 supplementation strongly enhanced the growth capability of pituitary stem cell organoids, thereby expanding their potential as experimental model.

Together, our study identifies IL-6 as pituitary stem cell activator upon local damage, a competence quenched at aging concomitant with raised IL-6/inflammatory level in the older gland. These new insights may open the way to interfering with pituitary aging.

Significance

The pituitary is the body's master endocrine gland. Local damage and aging present important threats. We started to decrypt the yet ill-defined regulation of the gland's stem cells, typically dormant but acutely activated upon damage. Single-cell transcriptomics uncovered interleukin-6 as pituitary stem cell activator upon local damage, corroborated *in vivo* and *in vitro* using stem cell-derived organoids. This competence extinguishes at aging, concurrent with raised

inflammatory state in the older gland (inflammaging). However, the aging pituitary's stem cells retain intrinsic activatability, re-surfacing once released from their impeding tissue milieu. Our new insights may instigate tactics to refrain the pituitary from aging, or rejuvenate the aging gland. The single-cell transcriptomic database provides a powerful resource to decipher pituitary damage and aging.

Introduction

The pituitary gland is the key orchestrator of the endocrine system, translating central and peripheral inputs into strictly regulated hormone outputs. Consequently, this master gland steers a multitude of fundamental processes including body growth, metabolism, sexual development, reproduction and stress management. To exert this crucial function, the pituitary encompasses specialized hormone-producing cell types, mainly located in the anterior lobe of the gland (anterior pituitary, AP) and comprising somatotropes (producing growth hormone (GH)), lactotropes (prolactin (PRL)), corticotropes (adrenocorticotropic hormone (ACTH)), gonadotropes (luteinizing hormone (LH) and/or follicle-stimulating hormone (FSH)) and thyrotropes (thyroid-stimulating hormone (TSH)). On top, the pituitary contains a population of stem cells, essentially marked by sex determining region Y-box 2 (SOX2) expression (1–4). The physiological role of the pituitary stem cells remains poorly understood (5, 6). Transgenic SOX2 lineage tracing revealed involvement in adult gland homeostasis and adaptation to altered endocrine demands, although contributions were not large (3, 4). Progressively, the picture emerges that adult pituitary stem cells are mainly dormant and not predominantly involved in tissue homeostasis and physiological remodeling (7–9), reminiscent of findings in other tissues with comparable low-turnover rates (such as muscle and liver; (10, 11)). Yet, in case of damage in the adult pituitary, the resident stem cell compartment shows swift activation (12, 13). More in particular, following diphtheria toxin (DT)-triggered endocrine cell-ablation injury in the GHCre/iDTR mouse model (expressing the Cre recombinase under control of the *Gh* promoter, as well as the Cre-inducible DT receptor (iDTR)), the pituitary stem cell population is promptly activated displaying enhanced proliferative activity and expansion (12). Substantial regeneration of the obliterated somatotropes is eventually observed after 5 to 6 months (12). Surprisingly, this regenerative competence of the gland rapidly

drops with aging, being not observed anymore when mice reach middle age (from 8-10 months of age; (14)).

Virtually nothing is known about the molecular machinery driving the quiescent pituitary stem cells into activation (as observed following local injury), neither about how this route may change at advancing age. In other tissues, it was found that stem cells undergo an intrinsic aging process (such as in the hematopoietic system; (15)), or regress in functionality because of the aging tissue milieu (as described in muscle and brain; (16–18)). Here, we started to tackle this query by interrogating young-adult and aging (middle-aged), damaged and undamaged pituitary (specifically, its major endocrine AP lobe) using single-cell transcriptomics. We focused on the prompt stem cell reaction that occurs immediately upon the DT-induced local damage in the GHCre/iDTR model, and substantiated transcriptomic findings using *in vivo* and *in vitro* exploration. To achieve the latter, we applied our recently developed mouse AP-derived organoid model (19). These organoids originate from the ($SOX2^{+}$) stem cells and maintain the pituitary stem cell phenotype in culture. Moreover, growth characteristics reflect the stem cells' activation (as observed following damage and at neonatal age), and organoid-based findings were found reliably translatable to the *in vivo* situation (19). Hence, this organoid system provides an interesting *in vitro* pituitary stem cell biology/activation readout tool.

In the present study, we identified interleukin-6 (IL-6) to be upregulated in the young pituitary following tissue injury, and uncovered its pituitary stem cell-activating competence, which however is quenched at aging concomitant with a raised inflammatory nature in the older gland. When released from the *in situ* microenvironment through organoid culturing, the aging pituitary's stem cells regain activatability. These new insights may be harnessed to combat pituitary aging and concomitant regenerative decline.

Results

Acute proliferative activation of the pituitary stem cells upon local injury subsides at aging

To controllably inflict injury in the pituitary, we used our previously designed GHCre/iDTR transgenic mouse model (12) (see Extended Methods). $GH^{Cre/+}$;$R26^{iDTR/+}$ mice (further referred to as GHCre/iDTR) and control $GH^{+/+}$;$R26^{iDTR/+}$ animals (further referred to as -/iDTR) were injected

with DT for 3 days, causing local tissue damage in the GHCre/iDTR pituitary by inducing apoptosis in endocrine cells (in particular, somatotropes and lactotropes; (12)). In accord with our previous findings (12), the resident SOX2^{+} stem cells of the young-adult pituitary (8-12 weeks old mice, further referred to as 'young') show an acute increase in proliferative activity (as assessed by Ki67 immunostaining; Fig. 1*A*) and ensuing expansion of SOX2^{+} cell number (*SI Appendix*, Fig. S1*A*). This prompt pituitary stem cell activation is significantly lower at older age (10-15 months old, middle-aged mice, further referred to as 'aging') (Fig. 1*A*; *SI Appendix*, Fig. S1*A*). In addition, the aging basal pituitary houses a reduced number of SOX2^{+} stem cells when compared to the young gland (*SI Appendix*, Fig. S1*A*), consistent with prior findings (14).

Recently, we established an *in vitro* organoid model starting from mouse pituitary (particularly, from the AP) which recapitulates biology and activation of the pituitary stem cells (19). The organoids develop from the SOX2^{+} stem cells as shown before for young AP (19), and demonstrated here for aging pituitary using SOX2$^{eGFP/+}$ reporter-mouse AP giving rise to only eGFP^{+} organoids (*SI Appendix*, Fig. S1*B*). In addition, when starting from a mixture of cells from SOX2$^{eGFP/+}$ and non-fluorescent wildtype (WT) aging AP, the developing organoids are either entirely fluorescent or non-fluorescent (*SI Appendix*, Fig. S1*B*), thereby supporting a clonal origin. Moreover, the organoids display a pituitary stemness phenotype in culture, both from young AP (see (19)) and from aging gland (*SI Appendix*, Fig. S1*C*), expressing known pituitary stem cell markers (SOX2, E-cadherin, cytokeratin-8/18; (19)), and showing absence of hormone-secretory granules and presence of microvilli, similar to the pituitary stem cells as present in the cleft-lining marginal zone (MZ) (*SI Appendix*, Fig. S1*D*). Using this model system as pituitary stem cell biology and activation readout (19), we observed that primary organoid formation efficiency (referred to as passage 0 or P0) from the aging pituitary is lower than from the young gland, and that the increase in organoid development capacity upon damage is less pronounced at the older age (Fig. 1*B*), both findings in line with the *in vivo* observations of regressed stem cell number and inferior activation response in aging *versus* young pituitary. Because the endocrine cell ablation in the damaged pituitary, together with the expansion of the SOX2^{+} cell population, entails that a higher absolute number of SOX2^{+} stem cells is seeded per well (i.e. per 10,000 AP

cells) from damaged than from undamaged gland, we determined the number of organoid-initiating SOX2$^+$ stem cells by normalizing for the calculated SOX2$^+$ cell numbers seeded (see Extended Methods). Similar conclusions were reached, showing an increase upon injury at both ages (indicative of stem cell activation), but again less prominent at older age (Fig. 1*C*).

Single-cell transcriptomics uncovers interleukin-6 to be upregulated in young pituitary upon damage

To in detail search for molecular underpinnings of the damage-induced pituitary stem cell response, and of the subsided reaction in the aging gland, we applied single-cell transcriptomics to the different pituitary conditions (i.e. young and aging, damaged and undamaged AP; Fig. 2*A*). After filtering out dead and low-quality cells, potential doublets and 'background' (ambient) RNA (*SI Appendix*, Fig. S2*A* and Extended Methods), applied collectively on all single-cell RNA sequencing (scRNA-seq) data obtained in this study (i.e. from young and aging, damaged and undamaged AP, in total yielding 26,115 good-quality cells), unsupervised clustering and visualization using Uniform Manifold Approximation and Projection (UMAP; (20)) were performed (*SI Appendix*, Fig. S2*B*). Subsequent superposition of canonical lineage markers exposed all known pituitary hormone-producing cell populations (Fig. 2*B*, Dataset S1 and *SI Appendix*, Fig. S2*B*). In addition, a connective tissue cluster (annotated in analogy to (21), and indicated with CT) and immune cell cluster were distinguished, as well as an endothelial and stem cell population, both subdivided in two subclusters (Fig. 2*B*). The endothelial cell subcluster 1 (EC1) shows more expression of mature endothelial cell markers than EC2 (Dataset S1 and *SI Appendix*, Fig. S2*C*), and a first basic mining of the stem cell population revealed that the subclusters (referred to as SC1 and SC2) differ in expression levels of several (pituitary) stemness markers (Dataset S1 and *SI Appendix*, Fig. S2*D*). Finally, a population of dying (apoptotic) cells was identified, being the result of the DT-induced apoptotic process in the GHCre/iDTR (damaged) AP, also included in the unsupervised clustering of the aggregate data (Fig. 2*A*-*C*). Of note, a small cluster of melanotrope cells (housed in the intermediate lobe (IL) of the pituitary) was also observed (Fig. 2*B*; *SI Appendix*, Fig. S2*B*), likely representing some limited IL tissue still attached to the AP after the latter's isolation from the mouse. Our cell-type

categorization outcome, as described above, was validated by performing the clustering based on regulon activity (i.e. transcription factors taken together with their positively regulated target genes) instead of based on differential gene expression (as in Fig. 2*B*), by applying 'single-cell regulatory network inference' (SCENIC; (22)). This alternative approach resulted in an analogous cell-type categorization pattern (*SI Appendix*, Fig. S2*E*). Moreover, integrating recently published pituitary scRNA-seq data of comparable mouse age, gender and strain (i.e. young wildtype C57/Bl6 male; (21, 23)) with our equivalent dataset showed prominent correlation (*SI Appendix*, Fig. S2*F*).

Looking deeper into the transcriptomic data of the stem cell population (Dataset S1), we detected, in addition to the well-known pituitary stem cell markers (*Sox2*, *Sox9*, *Cdh1*, *Krt8*, *Krt18*; *SI Appendix*, Fig. S2*D*; (19)), a number of interesting genes which we validated by *in situ* immunostaining analysis. *Tacstd2* (alias *Trop2*), found in stem cells of certain other tissues (24, 25), is within the AP stem cell population particularly expressed in SC1 (Dataset S1 and *SI Appendix*, Fig. S2*G*). *In situ*, TACSTD2/TROP2 protein expression was observed in the cleft-lining MZ stem cell compartment where it coincides with SOX2 (*SI Appendix*, Fig. S2*G*). Interestingly, TACSTD2 was not detected in the SOX2$^+$ cell groups in the AP parenchyma (*SI Appendix*, Fig. S2*G*), thereby providing an appealing marker to distinguish MZ from parenchymal stem cells (1, 2, 7). Of note, *Tacstd2* is also observed in the corticotrope cell cluster (Dataset S1 and *SI Appendix*, Fig. S2*G*). In agreement, TACSTD2 protein was detected in certain ACTH$^+$ cells, mainly located at the transition area between AP and IL (the so-called 'wedges'; (26)) (*SI Appendix*, Fig. S2*G*). Furthermore, the core Hippo pathway component *Yap1* was found highly expressed in the stem cell population (both SC1 and SC2; Dataset S1 and *SI Appendix*, Fig. S2*H*). In analogy, nuclear YAP$^+$ signal is present in SOX2$^+$ stem cells (both in the MZ and parenchyma) (*SI Appendix*, Fig. S2*H*), thereby expanding our previous findings (14) and confirming former studies that identified Hippo pathway activity in pituitary stem cells as particularly studied during embryonic and neonatal development (27, 28). *Yap1* expression is also seen in the connective tissue cluster, and in the endothelial cell clusters (Dataset S1 and *SI Appendix*, Fig. S2*H*) which is consistent with YAP reported in pituitary endothelial cells (27).

Finally, our scRNA-seq exploration revealed high and specific expression of *Cyp2f2* in the pituitary stem cell population (both SC1 and SC2; Dataset S1 and *SI Appendix*, Fig. S2*I*), in agreement with another recent pituitary scRNA-seq study (21). Here, we validated this expression and found that CYP2F2 is indeed localized in $SOX2^+$ stem cells (*SI Appendix*, Fig. S2*I*).

As described above, the pituitary stem cell population acutely reacts to local tissue damage, predominantly in the young gland. To search for molecular mechanisms underlying this acute injury response, we contrasted the stem cell transcriptomes of young damaged AP with undamaged gland using differentially expressed gene (DEG) and gene ontology (GO) analyses. Among the top DEGs, we found multiple inflammatory-related genes (e.g. *Cxcl10*, *Ifi27l2a*, *Ifitm3*, *Il6*, *Lcn2*, *Socs3*) that were upregulated following injury (Fig. 2*D,E* and Dataset S2). Accordingly, cytokine-/inflammatory response-related GO terms were enriched in the stem cell clusters upon damage (Fig. 2*F* and Dataset S3). Interestingly, within this context, the cytokine interleukin-6 (*Il6*) was found highly upregulated, particularly in subcluster SC1 (Fig. 2*D,E,G* and Dataset S2). *Il6* upregulation was also readily detected by RT-qPCR analysis in damaged *versus* undamaged AP (*SI Appendix*, Fig. S2*J*). Further scRNA-seq scrutiny showed that *Il6* expression is not only present in SC1, but also in the connective tissue cluster in which it also rises upon damage (Fig. 2*G* and Dataset S2). To validate the scRNA-seq expression pattern, we performed RNAscope *in situ* hybridization for *Il6*, *Sox2* and *S100a6*, a gene highly expressed in both stem cell and connective tissue clusters (Dataset S1 and *SI Appendix*, Fig. S2*K*). This *in situ* examination showed cellular overlap of the mRNA signals (Fig. 2*G*). Both stem cell and connective (supportive) tissue cells belong to the so-called folliculostellate (FS) cell group of the pituitary, a heterogeneous cell population in the past designated as local IL-6 source, and in rat marked by S100β (29–31). In analogy, S100A6 immunoreactivity is found in $SOX2^+$ stem cells of mouse pituitary, as well as in some non-$SOX2^+$ cells (*SI Appendix*, Fig. S2*K*). Finally, *Il6* gene expression is also detected in the endothelial cell population by scRNA-seq mining (Fig. 2*G* and Dataset S1), *in situ* also supported by RNAscope analysis showing *Il6* signal in a number of cells expressing the endothelial cell-specific plasmalemma vesicle associated protein (*Plvap*) (*SI Appendix*, Fig. S2*L*).

Interleukin-6 acts as a pituitary stem cell-activating factor at young age

Since IL-6 has been shown to activate stem cells in certain other tissues when upregulated upon local damage (such as in muscle and intestine; (32–34)), we addressed the question whether the cytokine may also act as pituitary stem cell-activating factor.

Adding IL-6 to organoid culture augments organoid formation efficiency from undamaged (young) AP (Fig. 3*A*), concomitant with proliferative activation of the organoid-driving stem cells (as analyzed by EdU incorporation; Fig. 3*B*). In contrast, IL-6 does not further enhance organoid formation from the damaged (young) gland (Fig. 3*A*) in which the stem cells are already activated and endogenous IL-6 levels elevated (see above; and as observed in the supernatant of starting organoid cultures (P0, day 3 of culture); Fig 3*C*).

The JAK/STAT pathway is a key downstream mediator of IL-6 signaling (35). IL-6 indeed augments the number of phosphorylated STAT3 (phospho-STAT3 or pSTAT3)-immunopositive cells in organoids from undamaged (young) AP, but not from damaged gland in which the $pSTAT3^+$ status is already high without IL-6 (Fig. 3*D*), advocating that the JAK/STAT pathway is activated in stem cells following the DT-induced tissue injury, as also supported by intense *Stat3* regulon activity in the damaged AP SC1 (*SI Appendix*, Fig S3*A*). Adding the STAT3 inhibitor STATTIC to AP cells from damaged gland largely blocks organoid formation indicating the importance of JAK/STAT signaling in this stem cell-driven process (Fig. 3*E*). Furthermore, supplementation of LMT-28, an antagonist of the IL-6 co-receptor gp130 (36), abolishes organoid formation (Fig. 3*E*). Along the same line, adding STATTIC and LMT-28 to undamaged AP cells counteracts the formation of organoids, with the stimulatory effect of IL-6 no longer being observed (Fig. 3*E*). Exposure of fully-grown organoids to LMT-28 results in a decrease in $pSTAT3^+$ cells and proliferative activity, and an increase in apoptosis (as analyzed by cleaved caspase 3 or CC3 immunostaining; *SI Appendix*, Fig. S3*B*), supporting that gp130/pSTAT3-mediated signaling is needed for stem cell proliferation and survival in the organoids. Taken

together, organoid read-out scrutiny indicates that IL-6 can act as pituitary stem cell activator and reveals the importance of the IL-6-associated JAK/STAT and gp130 signaling pathways in pituitary stem cell behavior.

To inspect whether IL-6 acts similarly *in vivo*, young WT mice were intraperitoneally (i.p.) injected with the cytokine and the effect on pituitary stem cell-proliferative activity analyzed. The proportion of proliferating SOX2^{+} stem cells is significantly elevated following IL-6 treatment, concomitant with an increase in pSTAT3^{+} cells in the SOX2^{+} cell population (Fig. 3*F*), together convincingly extrapolating the *in vitro* organoid-based findings to *in vivo*. Moreover, IL-6 injection generated a pituitary stem cell activation response in IL-6 knockout (KO; IL-6$^{-/-}$) mice, whereas a general inflammatory condition (as induced by CpG oligodeoxynucleotide (CpG) injection; (37)) did not (*SI Appendix*, Fig. S3*C*), demonstrating the specificity of the effect by IL-6 (independent of a general inflammatory reaction if any). Of note, CpG-induced inflammation in WT mice triggers a pituitary stem cell-proliferative reaction comparable to IL-6 (*SI Appendix*, Fig. S3*C*), in line with the upregulated systemic IL-6 levels as reported to occur in this model (37). Intriguingly, the SOX2^{+} stem cell population is not different in the IL-6 KO pituitary regarding number and quiescent (low-proliferative) status (*SI Appendix*, Fig. S3*D*). However, primary organoid formation from IL-6 KO AP is reduced (*versus* WT AP), and IL-6 KO organoids are not passageable (*SI Appendix*, Fig. S3*E*), indicating that endogenous IL-6 is important for these stem cell activities.

Finally, to determine whether IL-6, being upregulated in the pituitary after damage, is involved in the injury-induced stem cell activation, we applied anti-IL-6 antibody during the acute DT-triggered damage infliction in GHCre/iDTR mice (Fig. 3G). The stem cell-proliferative reaction is significantly reduced (Fig. 3G), coinciding with lowered pSTAT3^{+} cells in the AP (*SI Appendix*, Fig. S3*F*). Similarly, *in vivo* LMT-28 administration during damage infliction reduces the proportion of proliferating stem cells and pSTAT3^{+} cells in the AP (*SI Appendix*, Fig. S3*G*).

Taken all together, our data show that IL-6 is upregulated in young pituitary upon tissue damage and can act as pituitary stem cell-activating factor. In addition, they provide evidence that IL-6 is involved in the early stem cell activation reaction to injury.

IL-6 does not activate stem cells in the aging pituitary, which is typified by an elevated IL-6/inflammatory phenotype

In clear contrast to the observations in young mice, i.p. injection of IL-6 in aging animals does not trigger a stem cell-proliferative activation response (Fig. 4*A*). Intriguingly, basal *Il6* expression level was found higher in aging *versus* young (undamaged) AP (Fig. 4*B*), in particular in the stem cell subcluster SC1 (Fig. 4*C* and Dataset S4). DEG and GO analysis of the stem cell transcriptomes identified upregulation of cytokine-/inflammatory response-related terms and genes in the aging *versus* young (undamaged) pituitary SC1 (Fig. 4*C*-*E* and Dataset S3-4), and even more broadly in the whole AP (Fig. 4*E* and Dataset S3-4). In analogy, gene set enrichment analysis (GSEA) applied to the single-cell transcriptomic dataset revealed a striking enrichment of the 'inflammatory response' hallmark in aging *versus* young (undamaged) AP, and in particular also in its SC1 (Fig. 4*F*). Also, the 'IL-6/JAK/STAT3 signaling' hallmark is significantly enriched in aging *versus* young AP and stem cell population (Fig. 4*F*). In accordance, pSTAT3^{+} cells are more abundant in the aging pituitary (*SI Appendix*, Fig. S4*A*). Together, these findings indicate that the aging pituitary, including its stem cells, displays a basally higher IL-6/inflammatory status than the young gland, which may explain the absence of a stem-cell activation reaction in the older AP upon IL-6 administration (see Fig. 4*A*), and the inferior stem cell reaction to injury (see Fig. 1*A*). In support, injection of IL-6 does not further elevate the number of pSTAT3^{+} cells in the aging gland (*SI Appendix*, Fig. S4*B*). Moreover, inflicting pituitary damage in aging mice does not significantly increase *Il6* expression levels any further in the gland (*SI Appendix*, Fig. S4*C*) or its SC1 and connective tissue cluster (Dataset S5 and *SI Appendix*, Fig. S4*D*). A raised inflammatory nature at aging has also been found to occur in other organs, epitomized in the concept of inflammaging which states that a chronic low-grade inflammation gradually develops at progressing age, not only at the systemic but also organ level (38, 39), proposed to underlie deteriorating organ and stem cell functionality at aging (40–43). Regarding systemic signs of inflammaging, increased IL-6 level is the most clear and supported marker (38, 39). In agreement, we found significantly upregulated IL-6 plasma levels in aging mice when compared to young animals (Fig. 4*G*). Numbers of immune cells in the pituitary, encompassing resident and

infiltrated cells, are not altered in the aging animals (*SI Appendix*, Fig. S4*E*), similar to findings in the spleen (*SI Appendix*, Fig. S4*F*), thereby suggesting that the inflammaging process may still be subtle in the middle-aged (~1-year-old) animals when compared to elderly mice (~2 years) in which macrophage infiltration has been reported in certain organs (44, 45). Along the same line, plasma levels of (pro-)inflammatory cytokines other than IL-6, of which specifically TNF-α has been reported to be upregulated in elderly mice in some studies (38, 39), are not significantly changed (yet) in the middle-aged mice analyzed here (*SI Appendix*, Fig. S4*G*).

Taken together, our findings provide evidence that aging pituitary displays a raised IL-6/inflammatory phenotype which may underlie the declined stem cell activation upon injury or IL-6 exposure at aging.

Activatability of aging pituitary stem cells re-surfaces in organoid culture

Unexpectedly, in contrast to the absence of a stem cell-activating effect by IL-6 in the aging gland *in vivo* (Fig. 4*A*), we observed that IL-6 is able to increase the formation and proliferative activity of organoids from aging (undamaged) pituitary *in vitro* (Fig. 5*A*-*B*), concomitant with an elevation of pSTAT3^{+} cells (*SI* Appendix, Fig. *S*5*A*). We hypothesized that the elevated inflammatory status may swiftly disappear in culture when the stem cells are released from their old *in vivo* (micro-)environment. In support, as opposed to the upregulated IL-6/inflammatory response genes and hallmarks in aging pituitary and its stem cell clusters (see Fig. 4*E*-*F* and Dataset S3-4), expression of *Il6* and inflammatory response genes is not different anymore between aging and young pituitary stem cells once cultured *in vitro* in organoid conditions (analyzed at day 14 of P0 organoid culture; Fig. 5*C*).

Finally, in view of its pituitary stem cell-activating competence and importance for organoid culture as found in IL-6 KO conditions, we tested whether addition of IL-6 to organoid cultures prolongs their yet limited expandability (19). Indeed, administration of IL-6 significantly increased organoid passageability, from both young and aging, damaged and undamaged pituitary (Fig. 5*D*). Endogenous IL-6 expression and production was found to substantially decline during organoid culturing in subsequent passages (Fig. 5*E*; *SI* Appendix, Fig. *S*5*B*), plausibly underlying the before limited expandability in the absence of exogenous IL-6 supplementation. After long-

term passaging, organoids maintain their morphological and pituitary stem cell phenotype (as shown for damaged AP; *SI* Appendix, Fig. *S*5*C*).

Taken together, the aging pituitary's stem cells retain intrinsic activation capability which re-surfaces *in vitro* when liberated from the plausibly impeding IL-6/inflammatory stress *in vivo*. Moreover, achieving robust long-term expansion empowers the applicability of the organoid model system toward extensive exploration of pituitary stem cell biology and activation.

Discussion

In the present study, we searched for molecular mechanisms underlying the acute activation of adult pituitary stem cells upon local tissue injury, at present entirely unknown, and looked for differences with the aging gland, reported before to have lost damage-repair capacity (14). By applying single-cell transcriptomic profiling, we tracked down IL-6 as a factor that has the capacity to bring pituitary stem cells into activation mode. Back in 1989, we made the intriguing observation that a cytokine known for expression and function in the immune system (i.e. IL-6) was also expressed in an endocrine organ (i.e. the pituitary gland) (30, 46). IL-6 was found to be produced by the so-called FS cell population which represents a yet ill-defined, heterogeneous cell-type assembly in the pituitary, proposed to encompass paracrine-regulatory cells, physically supportive (connective tissue) cells, immune-associated cells and more recently, also stem cells (1, 2, 29, 31). Now 30 years later, our scRNA-seq interrogation eventually confirmed and refined the pituitary IL-6 source. The upregulation of IL-6 upon injury in the young gland, occurring particularly in the stem cell and connective tissue subsets, proposes a role, paracrine and/or autocrine, for these specific cell subpopulations in the injury-triggered stem cell activation (summarized in *SI* Appendix, Fig. *S*5*D*). *In vitro*, IL-6 was found to activate the pituitary stem cells resulting in more efficient organoid development, a newly developed tool to probe pituitary stem cell biology and activation (19). *In vivo*, IL-6 triggered acute pituitary stem cell activation in the young gland while blockade of IL-6 or associated signaling pathways strongly reduced the stem cell reaction at injury, together providing evidence that IL-6 is involved in the acute activation process of the quiescent pituitary stem cells in response to local tissue damage. Of note, Il-6 does not seem to be involved in the stem cell phenotype of the homeostatic gland which is not

changed in IL-6 KO mice, not illogical given the highly quiescent state of the stem cells in the basal gland, not in need of IL-6 action. It should be remarked that damage still induced some proliferative stem cell activation in the aging pituitary *in vivo* while IL-6 injection did not (Fig. 1*A* and Fig. 4*A*), and that the proliferative activation reached in young mice after damage appeared higher than after IL-6 injection (Fig. 1*A* and Fig. 3*F*). One explanation may be that local IL-6 levels in young pituitary after damage are higher than achieved after i.p. IL-6 injection. Furthermore, still other factors may additionally be involved in the stem cell activation process after injury (*SI* Appendix, Fig. *S*5*D*). Our scRNA-seq resource now provides an invaluable means to in-depth elucidate this molecular machinery, including the search for the upstream activators of IL-6 expression during damage.

Excitingly, our study demonstrates that the stem cells of aging pituitary regain activatability when removed from their *in vivo* tissue milieu. Hence, receded *in vivo* responsiveness and reaction to injury is not an intrinsic aging process of the pituitary stem cells, but may rather be imposed by an oppressive (inflammatory) microenvironment. Also in certain other tissues, it has been shown that stem cells retain their functional capacities at aging which is repressed by the environment (16–18, 47). Substituting the old milieu for a younger equivalent restored stem cell functionality in these tissues (18, 38, 47, 48). Taken together, we advance the concept (as summarized in *SI* Appendix, Fig. *S*5*D*) that the raised inflammatory environment in the aging pituitary, indicative of inflammaging, presents a roadblock for full activation of the resident stem cells upon injury. Or in other words, the prevailing IL-6/inflammatory milieu in the aging pituitary sets a threshold that is hard to surpass for unfolding an adequate acute reaction when challenged by injury. In the end, the subsided acute reaction of the stem cells may contribute to the absence of the later regeneration in aging pituitary upon cell-ablation injury (14). Indeed, it has been reported in other tissues that acute activation of the resident stem cells by IL-6 following insult represents a first essential step toward eventual repair (34, 49, 50). Definite evidence for an *in vivo* role of IL-6 in eventual pituitary regeneration awaits extensive and comprehensive scrutiny of GHCre/iDTR mice on the IL-6 KO background, ideally in a conditional (temporospatial), pituitary (stem/connective cell)-specific manner. Interestingly, it has been found that anti-inflammatory

intervention can restore regenerative capacity at aging in certain tissues (such as skin, muscle, liver, gut; (40–43)), an appealing path for future pituitary aging research. Finally, the present study strongly enlarges the applicability of our recently developed pituitary organoid model by effectively extending organoid expandability using IL-6, thus compensating for the decline of endogenous IL-6 production, which could be due to the disappearance of *in situ* stimulatory factors.

In conclusion, we identified and characterized IL-6 as pituitary stem cell activator, a competence quenched at aging concurrent with a raised IL-6/inflammatory stress level in the gland. Still, aging pituitary stem cells retain intrinsic stemness properties and show activatability when released from their *in vivo* microenvironment. These new insights may be instrumental to find strategies for restraining the master endocrine pituitary gland from aging, or for rejuvenating a burdened old gland. And more in general, our single-cell transcriptome database provides a rich source to search for processes underlying pituitary aging whose understanding is currently poor, and for potential therapeutic targets. In the end, IL-6 and inflammaging may represent appealing candidates.

Methods

Mice and *in vivo* treatments

GHCre/iDTR and control (-/iDTR) mice were injected with DT, and pituitaries (damaged and undamaged, respectively) collected (Fig. 2*A*). Young and/or aging mice were treated with IL-6, anti-IL-6 antibody, CpG or LMT-28 according to the indicated or described schedules. Further details are provided in *SI Appendix*.

Single-cell RNA sequencing

Damaged and undamaged AP from young and aging mice were dissociated into single cells (51, 52) and subjected to scRNA-seq analyses using 10x Genomics (Fig. 2*A*), according to manufacturer instructions. Libraries were sequenced and downstream analysis was performed in R using Seurat (53). Gene regulatory networks (regulons) were determined using SCENIC (22) in Python (pySCENIC). More details are given in *SI Appendix*.

Pituitary organoids

AP cells were plated in a drop of 70% Matrigel/30% serum-free defined medium (SFDM; Thermo Fisher Scientific), and pituitary organoid culture medium (19) was added. After growth (10-14 days), organoids were dissociated into small fragments which were re-seeded in Matrigel drops for passaging. More details are provided in *SI Appendix*.

Immunostaining

Whole pituitary and organoids were fixed and sections subjected to immunofluorescence staining (for antibodies, see *SI Appendix*, Table S1), or to transmission electron microscopy (see *SI Appendix*). Immunopositive-cell quantification and EdU labelling in organoids are described in *SI Appendix*.

RNAscope *in situ* hybridization

Whole pituitary was fixed and sections subjected to RNAscope analysis according to the manufacturer's recommendations (Advanced Cell Diagnostics). More details are provided in *SI Appendix*.

Gene expression analysis by RT-qPCR

RNA was reverse-transcribed (RT) and subjected to quantitative real-time PCR (qPCR) as previously described (19) using primers as listed in *SI Appendix*, Table S2. Further details are given in *SI Appendix*.

IL-6 measurement

IL-6 concentration was measured in organoid culture supernatant and mouse plasma using MSD (Meso Scale Discovery) kits according to the manufacturer's protocol (see *SI Appendix*).

Statistical analysis

Statistical analysis was performed using GraphPad Prism, as in detail described in *SI Appendix*. Statistical significance was defined as $P \leq 0.05$.

Acknowledgments

We thank Y. Van Goethem and V. Vanslembrouck for valuable technical help. We thank the VIB Nucleomics Core (in particular Rekin's Janky) and KU Leuven Genomics Core (particularly Álvaro Cortés Calabuig) for their expert assistance in scRNA-seq analysis, as well as Thomas Van Brussel and Bram Boeckx (D. Lambrechts' group, KU Leuven) for technical and bioinformatical support in scRNA-seq experiments, respectively. The computational resources used for scRNA-seq analysis were provided by the 'Vlaams Supercomputer Centrum' (VSC), managed by the 'Fonds Wetenschappelijk Onderzoek (FWO) – Vlaanderen'. We are also grateful to the Imaging Core (VIB, KU Leuven) and the Cell and Tissue Imaging Cluster (CIC; KU Leuven) for the use of microscopes, and the Center for Brain & Disease Research (CBD) Histology unit (VIB, KU Leuven) for the use of histology equipment. We acknowledge the use of the Electron Microscopy Platform (VIB, KU Leuven) and the Institute of Development, Aging and Cancer (Tohoku University, Sendai, Japan) for transmission electron microscopy.

Funding

This work was supported by several grants from the 'Bijzonder Onderzoeksfonds' (BOF) KU Leuven and from FWO – Vlaanderen, awarded to the principal investigators. A.V. (1141717N), E.L. (11A3320N), B.C. (11W9215N), A.J. (1158318N) and C.N. (1S14218N) are supported by a PhD Fellowship from the FWO/FWO-SB.

Competing financial interests

The authors declare no competing financial interests.

References

1. T. Fauquier, K. Rizzoti, M. Dattani, R. Lovell-Badge, I. C. A. F. Robinson, SOX2-expressing progenitor cells generate all of the major cell types in the adult mouse pituitary gland. *Proceedings of the National Academy of Sciences of the United States of America* **105**, 2907–12 (2008).
2. J. Chen, *et al.*, Pituitary progenitor cells tracked down by side population dissection. *Stem Cells* **27**, 1182–1195 (2009).
3. K. Rizzoti, H. Akiyama, R. Lovell-Badge, Mobilized adult pituitary stem cells contribute to endocrine regeneration in response to physiological demand. *Cell Stem Cell* **13**, 419–432 (2013).

4. C. L. Andoniadou, *et al.*, Sox2+ stem/progenitor cells in the adult mouse pituitary support organ homeostasis and have tumor-inducing potential. *Cell Stem Cell* **13**, 433–445 (2013).
5. H. Vankelecom, J. Chen, Pituitary stem cells: Where do we stand? *Molecular and Cellular Endocrinology* **385**, 2–17 (2014).
6. B. Cox, H. Roose, A. Vennekens, H. Vankelecom, Pituitary stem cell regulation: Who is pulling the strings? *Journal of Endocrinology* **234**, R135–R158 (2017).
7. H. Vankelecom, "Pituitary stem cells: Quest for hidden functions" in *Stem Cells in Neuroendocrinology*, D. Pfaff, Y. Christen, Eds. (Springer International Publishing, 2016), pp. 81–101.
8. X. Zhu, J. Tollkuhn, H. Taylor, M. G. Rosenfeld, Notch-dependent pituitary SOX2+ stem cells exhibit a timed functional extinction in regulation of the postnatal gland. *Stem Cell Reports* **5**, 1196–1209 (2015).
9. H. Roose, *et al.*, Major depletion of SOX2+ stem cells in the adult pituitary is not restored which does not affect hormonal cell homeostasis and remodelling. *Scientific Reports* **7**, 1–11 (2017).
10. A. S. Brack, T. A. Rando, Tissue-specific stem cells: Lessons from the skeletal muscle satellite cell. *Cell Stem Cell* **10**, 504–514 (2012).
11. A. Miyajima, M. Tanaka, T. Itoh, Stem/progenitor cells in liver development, homeostasis, regeneration, and reprogramming. *Cell Stem Cell* **14**, 561–574 (2014).
12. Q. Fu, *et al.*, The adult pituitary shows stem/progenitor cell activation in response to injury and is capable of regeneration. *Endocrinology* **153**, 3224–35 (2012).
13. Q. Fu, H. Vankelecom, Regenerative capacity of the adult pituitary: multiple mechanisms of lactotrope restoration after transgenic ablation. *Stem Cells and Development* **21**, 3245–57 (2012).
14. C. Willems, *et al.*, Regeneration in the pituitary after cell-ablation injury : time-related aspects and molecular analysis. *Endocrinology* **157**, 705–721 (2016).
15. D. J. Rossi, *et al.*, Cell intrinsic alterations underlie hematopoietic stem cell aging. *Proceedings of the National Academy of Sciences of the United States of America* **102**, 9194–9199 (2005).
16. M. B. Schultz, D. A. Sinclair, When stem cells grow old: Phenotypes and mechanisms of stem cell aging. *Development (Cambridge)* **143**, 3–14 (2016).
17. C. Domingues-Faria, M. P. Vasson, N. Goncalves-Mendes, Y. Boirie, S. Walrand, Skeletal muscle regeneration and impact of aging and nutrition. *Ageing Research Reviews* **26**, 22–36 (2016).
18. M. Segel, *et al.*, Niche stiffness underlies the ageing of central nervous system progenitor cells. *Nature* **573**, 130–134 (2019).
19. B. Cox, *et al.*, Organoids from pituitary as a novel research model toward pituitary stem cell exploration. *Journal of Endocrinology* **240**, 287–308 (2019).
20. L. McInnes, J. Healy, J. Melville, UMAP: Uniform manifold approximation and projection for dimension reduction (2018).
21. L. Y. M. Cheung, *et al.*, Single-cell RNA sequencing reveals novel markers of male pituitary stem cells and hormone-producing cell types. *Endocrinology* **159**, 3910–3924 (2018).
22. S. Aibar, *et al.*, SCENIC: Single-cell regulatory network inference and clustering. *Nature Methods* **14**, 1083–1086 (2017).
23. A. Mayran, *et al.*, Pioneer and nonpioneer factor cooperation drives lineage specific chromatin opening. *Nature Communications* **10**, 3807 (2019).
24. V. Fernandez Vallone, *et al.*, Trop2 marks transient gastric fetal epithelium and adult regenerating cells after epithelial damage. *Development* **143**, 1452–1463 (2016).
25. A. S. Goldstein, *et al.*, Trop2 identifies a subpopulation of murine and human prostate basal cells with stem cell characteristics. *Proceedings of the National Academy of Sciences of the United States of America* **105**, 20882–20887 (2008).
26. L. Gremeaux, Q. Fu, J. Chen, H. Vankelecom, Activated phenotype of the pituitary stem/progenitor cell compartment during the early-postnatal maturation phase of the gland. *Stem Cells and Development* **21**, 801–13 (2012).

27. E. J. Lodge, J. P. Russell, A. L. Patist, P. Francis-West, C. L. Andoniadou, Expression analysis of the Hippo cascade indicates a role in pituitary stem cell development. *Frontiers in Physiology* **7**, 1–11 (2016).
28. E. J. Lodge, *et al.*, Homeostatic and tumourigenic activity of SOX2+ pituitary stem cells is controlled by the LATS/YAP/TAZ cascade. *eLife* **8**, 1–26 (2019).
29. H. Vankelecom, Pituitary stem cells drop their mask. *Current Stem Cell Research & Therapy* **7**, 36–71 (2012).
30. H. Vankelecom, P. Carmeliet, J. van Damme, A. Billiau, C. Denef, Production of interleukin-6 by folliculo-stellate cells of the anterior pituitary gland in a histiotypic cell aggregate culture system. *Neuroendocrinology* **49**, 102–106 (1989).
31. W. Allaerts, H. Vankelecom, History and perspectives of pituitary folliculo-stellate cell research. *European Journal of Endocrinology* **153**, 1–12 (2005).
32. A. L. Serrano, B. Baeza-Raja, E. Perdiguero, M. Jardí, P. Muñoz-Cánoves, Interleukin-6 is an essential regulator of satellite cell-mediated skeletal muscle hypertrophy. *Cell Metabolism* **7**, 33–44 (2008).
33. P. Muñoz-Cánoves, C. Scheele, B. K. Pedersen, A. L. Serrano, Interleukin-6 myokine signaling in skeletal muscle: A double-edged sword? *FEBS Journal* **280**, 4131–4148 (2013).
34. K. A. Kuhn, N. A. Manieri, T. C. Liu, T. S. Stappenbeck, IL-6 stimulates intestinal epithelial proliferation and repair after injury. *PLoS ONE* **9**, 1–18 (2014).
35. S. Rose-John, Interleukin-6 family cytokines. *Cold Spring Harbor Perspectives in Biology* **10**, 1–18 (2018).
36. S.-S. Hong, *et al.*, A novel small-molecule inhibitor targeting the IL-6 receptor β subunit, glycoprotein 130. *The Journal of Immunology* **195**, 237–245 (2015).
37. E. Behrens, *et al.*, Repeated TLR9 stimulation results in macrophage activation syndrome like disease in mice. *Journal of Clinical Investigation* **121**, 2264-2277 (2011).
38. C. Franceschi, J. Campisi, Chronic inflammation (Inflammaging) and its potential contribution to age-associated diseases. *Journals of Gerontology - Series A Biological Sciences and Medical Sciences* **69**, S4–S9 (2014).
39. C. Franceschi, *et al.*, Inflamm-aging: An evolutionary perspective on immunosenescence. *Annals of the New York Academy of Sciences* **908**, 244–254 (2000).
40. J. Neves, P. Sousa-Victor, Regulation of inflammation as an anti-aging intervention. *FEBS Journal* **287**, 43–52 (2020).
41. J. Oh, *et al.*, Age-associated NF-κB signaling in myofibers alters the satellite cell niche and re-strains muscle stem cell function. *Aging* **8**, 2871–2896 (2016).
42. D. Jurk, *et al.*, Chronic inflammation induces telomere dysfunction and accelerates ageing in mice. *Nature Communications* **2** (2014).
43. J. Doles, M. Storer, L. Cozzuto, G. Roma, W. M. Keyes, Age-associated inflammation inhibits epidermal stem cell function. *Genes and Development* **26**, 2144–2153 (2012).
44. R. Büttner, *et al.*, Inflammaging impairs peripheral nerve maintenance and regeneration. *Aging Cell* **17** (2018).
45. R. Lu, N. K. Sampathkumar, B. A. Benayoun, “Measuring phagocytosis in bone marrow-derived macrophages and peritoneal macrophages with aging” in *Physiology & Behavior*, (2020), pp. 161–170.
46. H. Vankelecom, *et al.*, Immunocytochemical evidence that S-100-positive cells of the mouse anterior pituitary contain interleukin-6 immunoreactivity. *Journal of Histochemistry and Cytochemistry* **41**, 151–156 (1993).
47. I. M. Conboy, *et al.*, Rejuvenation of aged progenitor cells by exposure to a young systemic environment. *Nature* **433**, 760–764 (2005).
48. A. S. I. Ahmed, M. H. Sheng, S. Wasnik, D. J. Baylink, K.-H. W. Lau, Effect of aging on stem cells. *World Journal of Experimental Medicine* **7**, 1 (2017).
49. E. Galun, S. Rose-John, “The regenerative activity of Interleukin-6” in *Tissue-Protective Cytokines: Methods and Protocols*, (2013), pp. 59–77.
50. T. Tadokoro, *et al.*, IL-6/STAT3 promotes regeneration of airway ciliated cells from basal stem cells. *Proceedings of the National Academy of Sciences of the United States of America* **111**, 3641–3649 (2014).

51. C. Denef, E. Hautekeete, A. de Wolf, B. Vanderschueren, Pituitary basophils from immature male and female rats: distribution of gonadotrophs and thyrotrophs as studied by unit gravity sedimentation. *Endocrinology* **103**, 724–735 (1978).
52. B. van der Schueren, C. Denef, J.-J. Cassiman, Ultrastructural and functional characteristics of rat pituitary cell aggregates. *Endocrinology* **110**, 513–523 (1982).
53. A. Butler, P. Hoffman, P. Smibert, E. Papalexi, R. Satija, Integrating single-cell transcriptomic data across different conditions, technologies, and species. *Nature Biotechnology* **36**, 411–420 (2018).

Legends to Figures

Fig. 1. Pituitary stem cell activation following tissue injury subsides at aging. *(A)* Immunofluorescence staining of SOX2 (magenta) and Ki67 (green) in basal (undamaged) and damaged anterior pituitary (AP)-derived cytospin samples of young and aging mice. Nuclei are labeled with Hoechst33342 (blue). Arrowheads indicate double-immunopositive cells. (Scale bar, 50 μm.) Bar graphs show the proportion of $SOX2^+Ki67^+$ cells in $SOX2^+$ cells (mean ± SEM), and the fold change in absolute $SOX2^+Ki67^+$ cell number (mean ± SEM) after damage (i.e. relative to undamaged AP, set as 1 (dashed line)) (for calculation of absolute cell numbers, see Extended Methods in *SI Appendix*). Data points represent biological replicates. $^*P \leq 0.05$; $^{**}P \leq 0.01$; $^{***}P \leq 0.001$; $^{****}P \leq 0.0001$. *(B)* Organoid formation efficiency from undamaged and damaged, young and aging AP. Representative bright-field pictures of organoid cultures are shown (passage 0, P0; scale bar, 500 μm.) Bar graphs indicate number of organoids developed and fold change in organoid number after pituitary damage (relative to undamaged AP) (mean ± SEM). Data points represent biological replicates. $^*P \leq 0.05$; $^{**}P \leq 0.01$. *(C)* Percentage of organoid-initiating $SOX2^+$ cells per well of 10,000 seeded AP cells from the conditions as indicated. Bar graphs show mean ± SEM and data points represent biological replicates. $^*P \leq 0.05$.

Fig. 2. Single-cell transcriptomic profiling reveals upregulation of interleukin-6 in young pituitary following tissue injury. *(A)* Experimental schematic for the scRNA-seq analysis. DT, diphtheria toxin; AP, anterior pituitary; IL, intermediate lobe; PP, posterior pituitary. Mouse icon obtained from freepik.com. *(B)* UMAP plot of the annotated cell clusters in the aggregate AP samples (i.e. collective single-cell transcriptome datasets from young and aging, undamaged and damaged AP). Somato, somatotropes; Lacto, lactotropes; Cortico, corticotropes; Gonado, gonadotropes; Thyro, thyrotropes; Melano, melanotropes; SC1 and SC2, stem cell cluster 1 and 2; EC1 and EC2, endothelial cell cluster 1 and 2; Immune, immune cells; CT, connective tissue cells; Apoptotic, apoptotic cells. *(C)* UMAP plot of undamaged and damaged AP (young and aging combined). *(D)* Heatmaps displaying the scaled expression of inflammatory response genes in the stem cell clusters SC1 and SC2 of young undamaged and damaged AP. *(E)* Volcano plot

displaying DEGs in SC1 of young AP. Colored dots represent significantly up- (orange) and down- (green) regulated genes in damaged *versus* undamaged AP. A selection of genes (as mentioned in the text) is indicated, and interleukin-6 (Il6) is highlighted. *(F)* Significant (FDR ≤ 0.05) DEG-associated GO terms linked with inflammatory processes enriched in SC1 and SC2 of young damaged *versus* undamaged AP. *(G)* Violin plot (top) and projection on UMAP diagram (bottom) of *Il6* expression in young undamaged and damaged AP with indication of relevant cell clusters. Triple RNAscope *in situ* hybridization analysis of young (undamaged) AP for *Sox2* (cyan), *Il6* (magenta) and *S100a6* (yellow). Boxed areas are magnified. Nuclei are stained with DAPI (blue). Arrowheads indicate cells with colocalized expression. (Scale bar, 50 µm.)

Fig. 3. IL-6 acts as pituitary stem cell-activating factor at young age. *(A)* Organoid development from undamaged and damaged young AP in the absence (control, CTRL) or presence of IL-6 (P0; scale bar, 500 µm.) Bar graphs show number of organoids formed (mean ± SEM). Data points represent biological replicates. $^{*}P \leq 0.05$. *(B)* Proliferative activity of organoids grown in the absence (CTRL) or presence of IL-6 (P0), as assessed by EdU incorporation (green). Nuclei are stained with Hoechst33342 (blue). (Scale bar, 50 µm.) Bar graph shows percentage of EdU^{+} cells in organoids (mean ± SEM). Data points represent individual organoids from 3 biological replicates. $^{****}P \leq 0.0001$. (*C*) IL-6 protein levels in supernatant of organoid cultures (P0, day 3 of culture) from young undamaged and damaged AP. Bar graph shows mean ± SEM and data points represent biological replicates. $^{*}P \leq 0.05$. *(D)* Immunofluorescence staining of pSTAT3 (green) in young AP organoids grown in the absence (CTRL) or presence of IL-6 (P0). Nuclei are stained with Hoechst33342 (blue). (Scale bar, 100 µm.) Bar graphs show percentage of $pSTAT3^{+}$ cells in organoids (mean ± SEM). Data points represent biological replicates. $^{**}P \leq 0.01$. *(E)* Organoid development from young damaged AP treated as indicated (P0; scale bar, 500 µm.) Bar graphs show number of organoids formed (mean ± SEM) from young damaged and undamaged AP under conditions as indicated. Data points represent biological replicates. $^{*}P \leq 0.05$. *(F)* Time schedule of *in vivo* treatment with IL-6. Immunofluorescence staining of SOX2 (magenta) and Ki67 (green) in basal (undamaged) AP-derived cytospin samples of young

wildtype (WT) mice, *in vivo* injected with IL-6 or vehicle (CTRL). Nuclei are labeled with Hoechst33342 (blue). Arrowheads indicate double-immunopositive cells. (Scale bar, 50 μm.) Bar graphs show percentage of $SOX2^{+}Ki67^{+}$ or $SOX2^{+}pSTAT3^{+}$ cells in $SOX2^{+}$ cells (mean ± SEM) and data points represent biological replicates. *$P \leq 0.05$. *(G)* Time schedule of *in vivo* treatment with anti-IL-6 antibody (IL-6 Ab). Bar graph shows percent change (relative to CTRL with mean set to 100%) of $SOX2^{+}Ki67^{+}$ cells in $SOX2^{+}$ cells (determined using cytospin samples) in the AP of young mice subjected to DT-induced damage infliction, and simultaneously treated with IL-6 Ab (mean ± SEM). Data points represent biological replicates. *$P \leq 0.05$.

Fig. 4. IL-6 does not activate stem cells in aging pituitary which displays an elevated IL-6/inflammatory phenotype. *(A)* Time schedule of *in vivo* treatment with IL-6. Immunofluorescence staining of SOX2 (magenta) and Ki67 (green) in basal (undamaged) AP-derived cytospin samples of aging WT mice, *in vivo* injected with IL-6 or vehicle (CTRL). Nuclei are labeled with Hoechst33342 (blue). Arrowheads indicate double-immunopositive cells. (Scale bar, 50 μm.) Bar graph shows percentage of $SOX2^{+}Ki67^{+}$ cells in $SOX2^{+}$ cells (mean ± SEM) and data points represent biological replicates. *(B) Il6* gene expression in aging *versus* young basal (undamaged) AP as determined by RT-qPCR. Bar graph shows fold change in aging AP relative to young (mean ± SEM) and data points represent biological replicates. **$P \leq 0.01$. *(C)* Volcano plot displaying DEGs in SC1 in young and aging undamaged AP. Colored dots represent significantly up- (blue) and down- (pink) regulated genes in aging *versus* young AP. A selection of genes is indicated, and Il6 is highlighted. *(D)* Significant (FDR ≤ 0.05) DEG-associated GO terms linked with inflammatory processes enriched in the stem cell cluster SC1 of aging *versus* young (undamaged) AP. *(E)* Heatmap displaying the fold change (presented as -logFC) of inflammatory response genes up- (blue) and down- (pink) regulated at aging. *(F)* GSEA analysis of ‘inflammatory response’ and ‘IL-6/JAK/STAT3’ hallmarks in aging compared to young (undamaged) AP and its SC1 and SC2, visualized as normalized enrichment score (NES). **FDR ≤ 0.01; ****FDR ≤ 0.0001; ns, non-significant. *(G)* Systemic plasma levels of IL-6 in young and

aging WT (undamaged) mice. Bar graph shows mean ± SEM, and data points represent biological replicates. *$P \leq 0.05$.

Fig. 5. Aging pituitary's stem cells regain activatability to IL-6 in organoid culture. *(A)* Organoid development from undamaged and damaged aging AP in the absence (CTRL) or presence of IL-6 (P0; scale bar, 500 µm.) Bar graphs show number of organoids formed (mean ± SEM). Data points represent biological replicates. *$P \leq 0.05$. *(B)* Proliferative activity of organoids grown in the absence (CTRL) or presence of IL-6 (P0), as assessed by EdU incorporation (green). Nuclei are stained with Hoechst33342 (blue). (Scale bar, 50 µm.) Bar graph shows percentage of EdU^+ cells in organoids (mean ± SEM). Data points represent individual organoids from 3 biological replicates. **$P \leq 0.01$. *(C)* Expression levels of *Il6*/inflammatory response genes in organoid culture (P0, day 14) from aging and young (undamaged) AP as determined by RT-qPCR (mean ± SEM). Data points represent biological replicates. *(D)* Bar graphs showing the (maximum) number of AP organoid passage at present reached, grown in the absence (CTRL) or presence of IL-6 (mean ± SEM). Data points represent biological replicates. *$P \leq 0.05$; **$P \leq 0.01$; ****$P \leq 0.0001$. *(E) Il6* gene expression levels in organoids from young and aging (damaged) AP at consecutive passages (each at day 14 of culture) as determined by RT-qPCR. Bars show mean ± SEM and data points represent biological replicates. *$P \leq 0.05$; **$P \leq 0.01$.